



# Pedogenic weathering and relative age dating of Quaternary alluvial sediments in the Pindus Mountains of northwest Greece

[Link to publication record in Manchester Research Explorer](#)

## Citation for published version (APA):

Woodward, J. C., Macklin, M. G., Lewin, J., Robinson, D. A. (Ed.), & Williams, R. B. G. (Ed.) (1994). Pedogenic weathering and relative age dating of Quaternary alluvial sediments in the Pindus Mountains of northwest Greece. In *Rock Weathering and Landform Evolution* (pp. 259-283). John Wiley & Sons Ltd.

## Published in:

Rock Weathering and Landform Evolution

## Citing this paper

Please note that where the full-text provided on Manchester Research Explorer is the Author Accepted Manuscript or Proof version this may differ from the final Published version. If citing, it is advised that you check and use the publisher's definitive version.

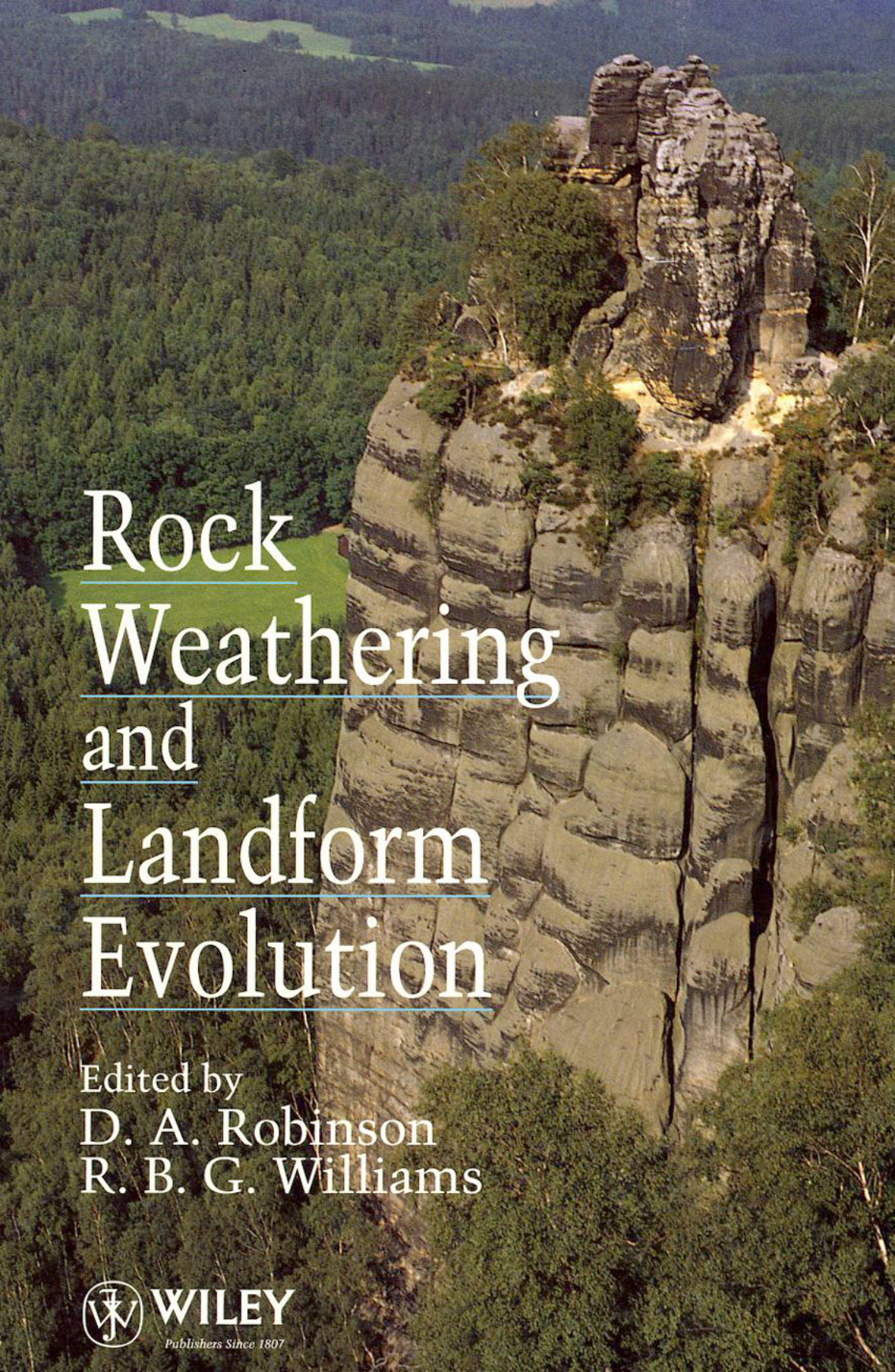
## General rights

Copyright and moral rights for the publications made accessible in the Research Explorer are retained by the authors and/or other copyright owners and it is a condition of accessing publications that users recognise and abide by the legal requirements associated with these rights.

## Takedown policy

If you believe that this document breaches copyright please refer to the University of Manchester's Takedown Procedures [<http://man.ac.uk/04Y6Bo>] or contact [uml.scholarlycommunications@manchester.ac.uk](mailto:uml.scholarlycommunications@manchester.ac.uk) providing relevant details, so we can investigate your claim.





# Rock Weathering and Landform Evolution

Edited by  
D. A. Robinson  
R. B. G. Williams



**WILEY**

*Publishers Since 1807*

---

# Rock Weathering and Landform Evolution

---

*Edited by*

**D. A. Robinson**

*and*

**R. B. G. Williams**

*Geography Laboratory  
University of Sussex, Brighton, UK*

Copyright © 1994 by John Wiley & Sons Ltd,  
Baffins Lane, Chichester,  
West Sussex PO19 1UD, England  
Telephone National Chichester (0243) 779777  
International (+44) (243) 779777

All rights reserved.

**JOHN WILEY & SONS**

Chichester · New York · Brisbane · Toronto · Singapore

---

# 16 Pedogenic Weathering and Relative-age Dating of Quaternary Alluvial Sediments in the Pindus Mountains of Northwest Greece

---

**JAMIE C. WOODWARD**

*Manchester Metropolitan University, UK*

**MARK G. MACKLIN**

*University of Leeds, UK*

and

**JOHN LEWIN**

*UCW Aberystwyth, UK*

## ABSTRACT

A chronosequence of soil profiles is described from the terraced alluvial sediments of the Voidomatis River in northwest Greece. Pedogenic weathering and profile development include increases in soil depth, organic matter translocation, leaching of calcium carbonate, clay illuviation, oxidation of ferrous iron minerals and changes in the magnetic susceptibility of different soil horizons. The pedogenic weathering data form several relative-age indicators which are used to supplement the interpretation of the primary depositional record for the basin. It is concluded that the northern Pindus mountains were probably glaciated before the last major (Late Würm) ice advance and that at least two major phases of glacial activity can now be recognised in the Greek Pleistocene.

## INTRODUCTION

The study of pedogenic weathering and soil formation is of fundamental importance to geomorphology. A detailed understanding of the processes and products of mineral weathering is an essential requirement for both contemporary studies of material transfer and for longer-term investigations of sediment diagenesis and landsurface lowering. In many environments, prior to entering a mass movement or fluid transport system, sediment will reside in a soil system and it is the processes of weathering and pedogenesis operating there which largely control the quality of solutes and sediments eventually transported from an area (Statham, 1977). Even though many of these processes act only very slowly, pedogenic weathering forces the alteration and mobilisation of surficial materials and is thus a major element in the relief-forming

mechanisms of any climatic zone (cf. Büdel, 1982). It is also apparent that the study of pedogenic weathering profiles is a most useful tool for investigating landscape history and environmental change, especially during the Quaternary Period (Birkeland, 1984; Catt, 1986; Bull, 1991).

During pedogenesis, as mineral breakdown proceeds and solute and particle transfers take place, weathering profiles can stockpile a variety of environmental clues. Consequently soil profiles, and especially soil chronosequences, offer a rich source of information on rates and processes of mineral weathering and may aid in establishing regional chronologies for Quaternary landform development. Soils have provided a major input to many palaeoenvironmental investigations in three main ways: (1) As soils represent episodes of relative geomorphological stability, they mark the position of buried or relict landsurfaces (e.g. Kukla, 1987), and may assume considerable stratigraphical importance over wide areas (e.g. Rose *et al.*, 1985). (2) Their weathering products are often preserved in sufficient detail to form a record of the environmental conditions responsible for their formation—thus providing useful information that cannot be obtained from the primary depositional record (Kemp, 1987). (3) Since many pedogenic features can be related to profile maturity, soils can be used as a means of relative-age dating (e.g. Birkeland, 1982; McFadden and Hendricks, 1985; Colman and Pierce, 1986). Furthermore, in the absence of datable materials and diagnostic fossils, evidence obtained from pedogenic weathering may provide the only available means of differentiating between otherwise similar deposits. The last two decades have witnessed both a growing awareness of the value of such data sources and an ever increasing number of researchers seeking to integrate information from soil profiles into more traditional, primary-sediment-based studies of the Quaternary rock record (cf. Birkeland, 1984; Boardman, 1985; Weide, 1985; Bull, 1991).

The authors have recently conducted detailed field investigations in the Voidomatis River basin of northwest Greece in order to establish the nature of the Quaternary sedimentary record. This work formed part of a wider geoarchaeological survey of Late Quaternary environmental change and Palaeolithic settlement, allied to recent excavations at the Klithi rockshelter (Bailey *et al.*, 1984 and 1986). While the alluvial sequence provided the main focus for our initial investigations (Lewin *et al.*, 1991; Woodward *et al.*, 1992), the project also included an investigation of soil profile development in the terraced alluvial sediments of the Voidomatis River. These terrace surfaces are generally well preserved, forming prominent landscape features throughout most of the catchment. This chronosequence presented a rare opportunity to observe patterns of pedogenic weathering and soil profile genesis during the late Quaternary in a hitherto little studied region of southern Europe.

In terms of Quaternary landform development, the region is of particular interest as it represents one of the most southerly locations in Europe with evidence of extensive Pleistocene glacial activity (Woodward, 1990). Furthermore, the annual rainfall currently exceeds 2000 mm, and climatic conditions in this humid alpine Mediterranean zone promote comparatively rapid rates of pedogenic weathering by most European standards. This paper summarises the results of our soil profile work by describing the nature of the pedogenic weathering regime and illustrating the use of several relative-age indicators to supplement and refine our interpretation of the primary depositional record.

## GEOLOGICAL AND GEOMORPHOLOGICAL SETTING

### The Voidomatis Basin

The study area is situated in the Epirus region of northwest Greece approximately 40 km northeast of the provincial capital of Ioannina. The Voidomatis River (384 km<sup>2</sup>) drains part of the high-relief karst terrain of the Pindus Mountain Range (Figures 16.1 and 16.2). Elevations within the basin range from <450 m on the Konitsa Plain (Figure 16.3) to over 2400 m along the watershed of the Voidomatis and Aoos Rivers. The catchment is developed in resistant Jurassic and Eocene limestones which are capped in places by thick flysch deposits of Late Eocene to Miocene age. The hard limestone rocks support the formation of deep gorges and steep-sided tributary ravines (Figure 16.2). In contrast, the erodible flysch deposits support sub-catchments of lower relief with comparatively higher drainage densities and present-day suspended sediment yields. The physiography of the catchment is presented in greater detail in Woodward *et al.* (1992). The five soil profiles under discussion are located along a 6 km reach of the Voidomatis River which incorporates all of the Lower Vikos Gorge (Vikos to Old Klithonia Bridge) and the most southerly part of the Konitsa Plain (Figures 16.1 and 16.2).

### Climatic Regime

The Pindus Mountains trend roughly NNW–SSE and lie parallel to the modern Ionian coastline of northwest Greece. The Epirus region contains many of the highest mountains in Greece with several peaks exceeding 2400 m. These mountains present a major relief barrier to the convectively unstable, moisture-laden air masses associated with the Mediterranean winter, and the study area falls within the 'Mountain climate' zone of Walter and Lieth (1960), and is located on the boundary between the 'Rain all year' and 'Winter and Autumn' Mediterranean rainfall regimes described by Huttary (1950). Mean annual rainfall frequently exceeds 2000 mm (Furlan, 1977). The summer months are generally hot and dry although heavy thunderstorms are not uncommon during July and August. Mean July temperatures of 15°C are typical in the highest central belt of the northern Pindus Mountains and this may rise to 20°C at intermediate altitude.

### The Quaternary Alluvial Sequence in the Voidomatis Basin

The alluvial deposits and landforms of the Voidomatis River have recently been described in detail by Lewin *et al.* (1991). This work documents five major Quaternary alluvial units (Figure 16.1) and their major features are summarised in Table 16.1. The weathering profiles developed on the terraced alluvial units which postdate the Kipi unit form the basis of this study. From the information presented in Table 16.1 and Figure 16.4 it is clear that these alluvial units are not of uniform composition. Lithological contrasts are apparent in both the coarse (8–256 mm) and fine (<63 µm) elements of the parent alluvial sediments, and these result from a series of marked shifts in catchment sediment sources which took place during the Late Quaternary (Woodward *et al.*, 1992) and are briefly described below.

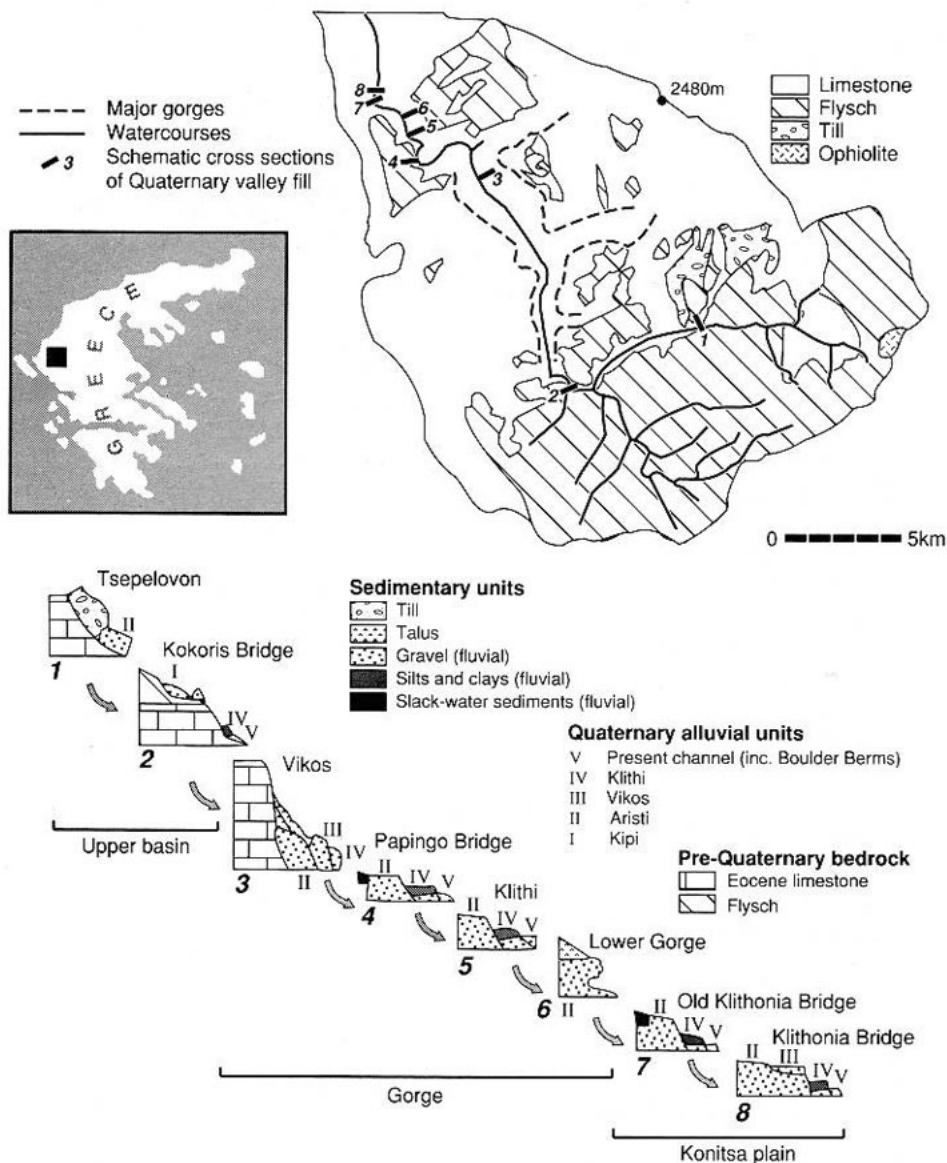


**Figure 16.1** A simplified geological and drainage map of the Voidomatis River basin showing the location of eight key sites where the stratigraphic relationships in the Quaternary alluvial sequence are particularly well exposed. The lower diagram shows schematic sections of the alluvial succession and associated terrace surfaces at each of these sites. Site 1 is located approximately 1.5 km south of the village of Tspelovon in the glaciated portion of the catchment. The main Vikos Gorge lies between Kokoris Bridge (2) and Vikos (3), and the Lower Vikos Gorge lies between Vikos (3) and the Old Klithonia Bridge (7). The Voidomatis River joins the Aoo River approximately 5 km north of site 7

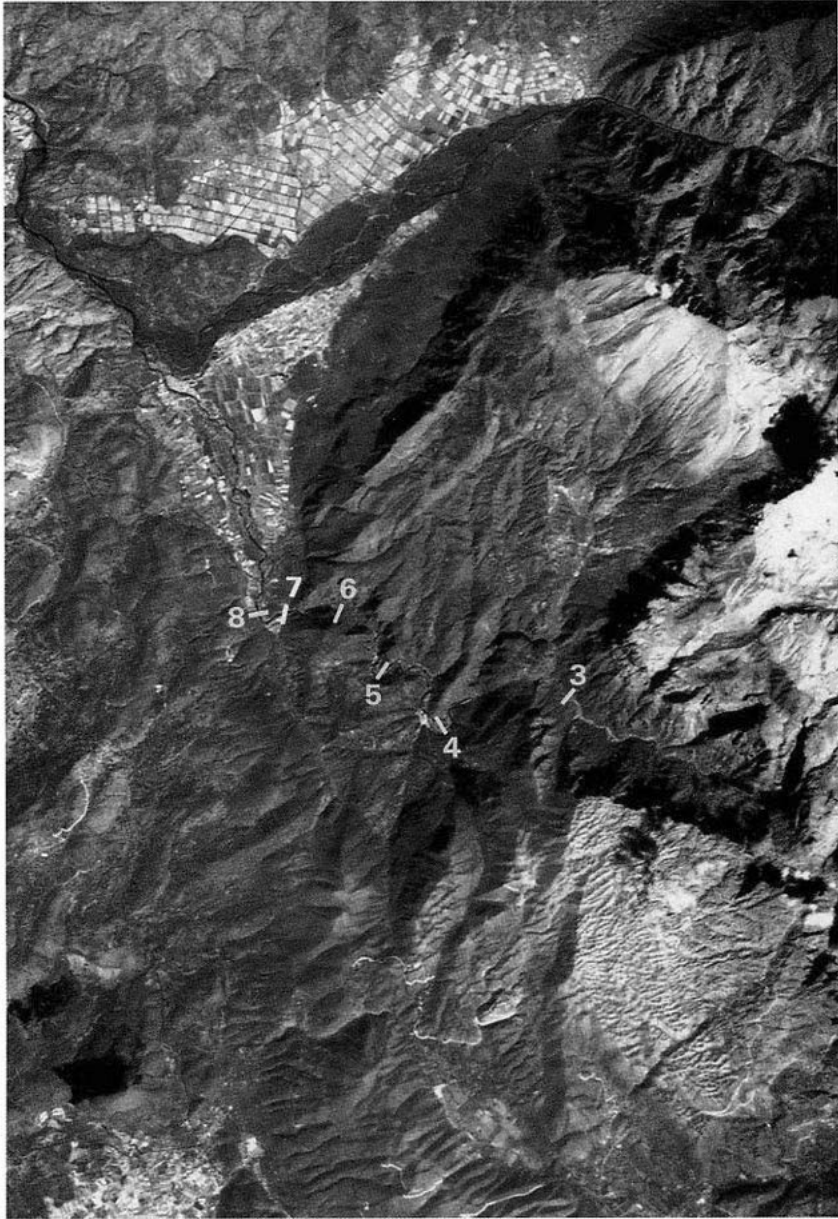


**Figure 16.2** SPOT satellite image of the Lower Vikos Gorge and the Konitsa Plain to illustrate the high-relief, block-faulted terrain of the study region. The western end of the Vikos Gorge is also shown and six of the sites shown in Figure 16.1 are also indicated. This scene covers an area of approximately  $20 \text{ km} \times 14 \text{ km}$ . The Voidomatis and Aonos Rivers both exit fault-bounded limestone gorges onto the Konitsa Plain and their confluence is approximately 10 km from the Albanian border



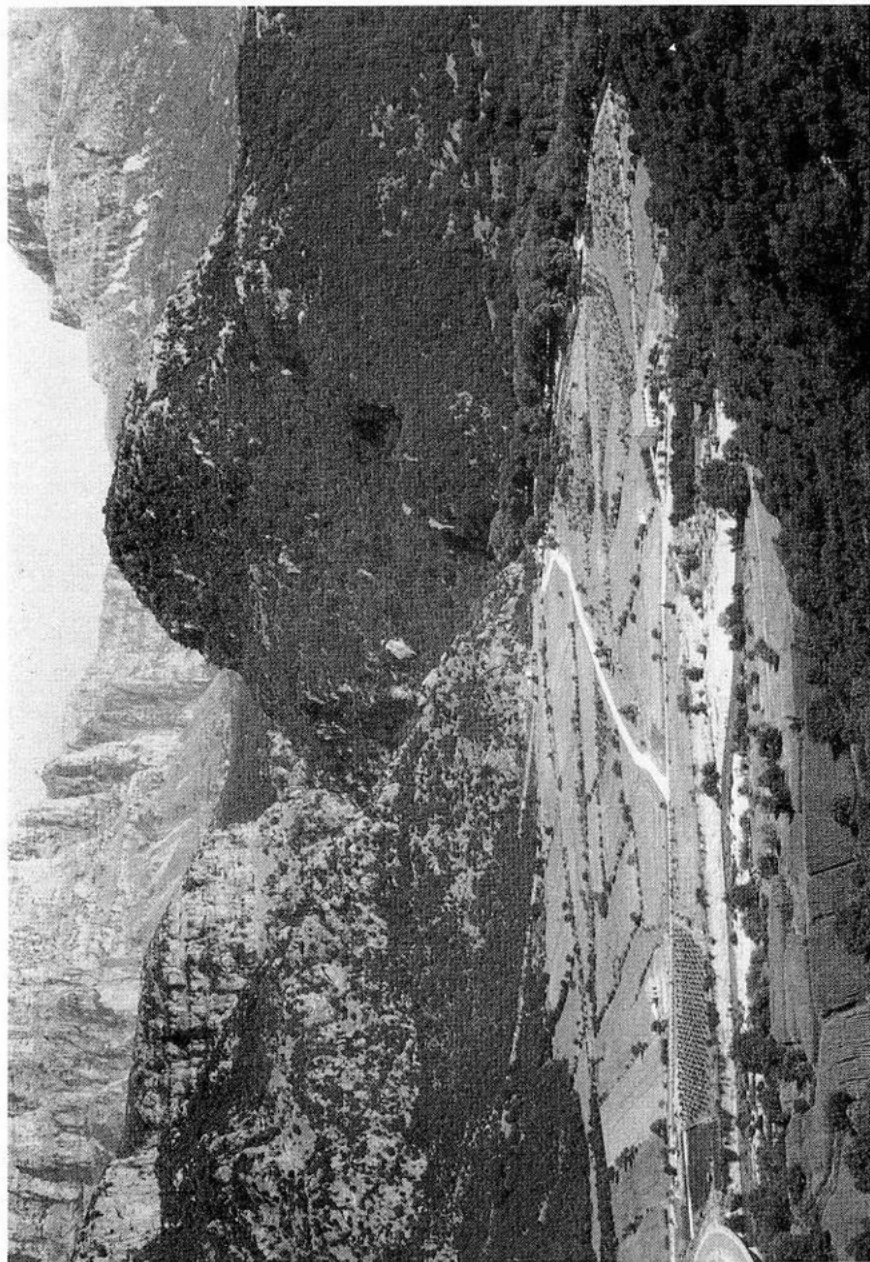


**Figure 16.3** The southern part of the Konitsa Plain looking upstream (eastwards) into the Lower Vikos Gorge with the western end of the Vikos Gorge in the background. The course of the modern stream is marked by the line of trees to the right. Soil profiles B and D are located 40 m and 100 m respectively downstream of the end of the Lower Vikos Gorge. An 8 m high right-bank section in Aristi unit gravels is shown in the middle of this photograph

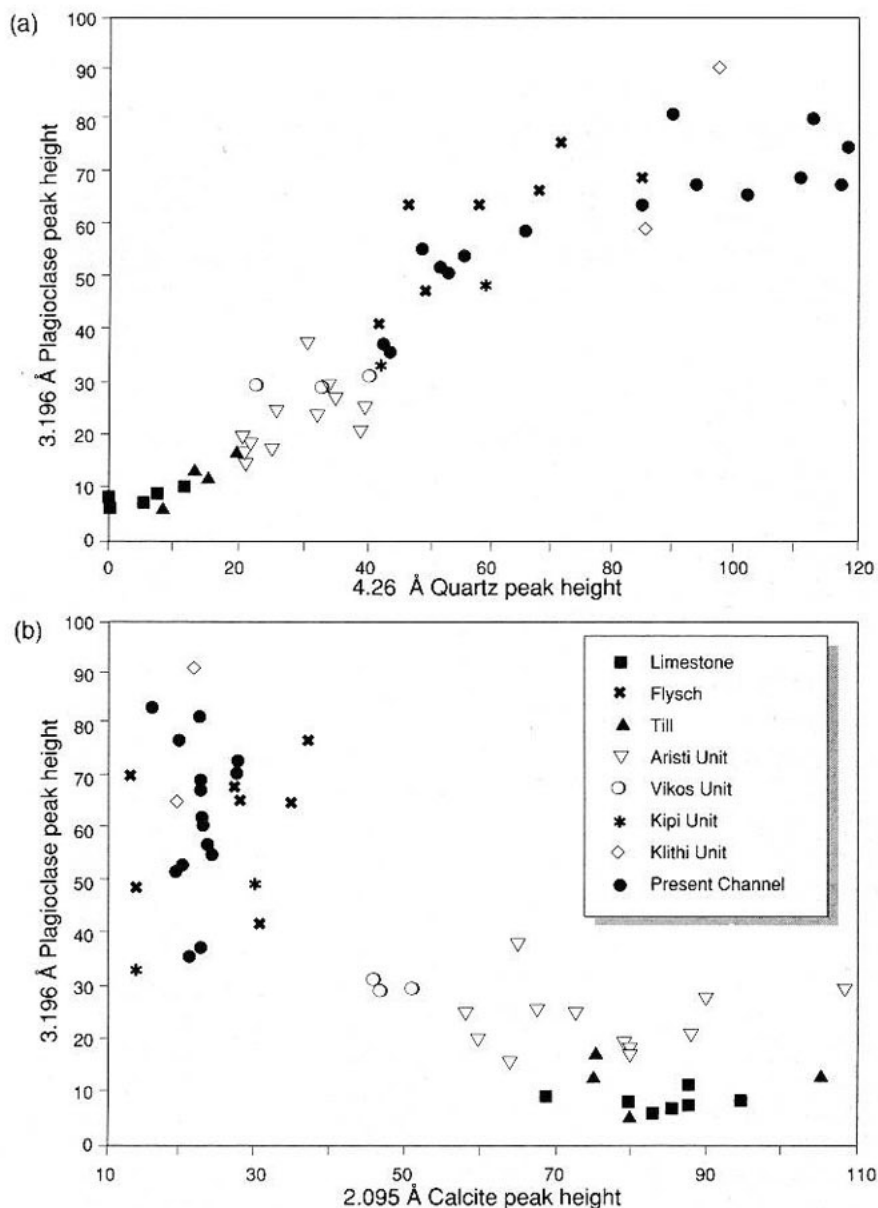


**Figure 16.4** Peak height data from X-ray diffraction traces showing the broad mineralogical composition of the  $<63 \mu\text{m}$  component of the parent alluvial sediments. (a) Plot showing the strong positive correlation between quartz and plagioclase in the basin parent materials. (b) Plot showing calcite and plagioclase relationships. The Aristi unit sediments (soil profiles A and B) are poor in plagioclase and quartz and rich in calcite reflecting their origin from limestone-rich glacial (till) sediments. In contrast the Klithi unit sediments (soil profiles D and E) are rich in non-carbonate (flysch-derived) materials. The Vikos unit sediments (soil profile C) are intermediate between these two groups

**Table 16.1** Altitudinal relationships, lithological properties, depositional environments (including major suspended sediment sources) and ages of the Quaternary alluvial units in the Voidomatis basin. The dates were obtained by the following methods: a) AMS  $^{14}\text{C}$ ; b) ESR; c) Thermoluminescence

| Alluvial unit   | Height of terrace surface above river bed level (m) | Maximum observed thickness of unit (m) | Clasts <i>N</i> | Samples <i>N</i> | Clast lithological (bedload) composition (8–256 mm) |          |         |             |
|-----------------|---|--|-----------------|------------------|---|----------|---------|-------------|
|                 |   |  |                 |                  | % Limestone   | % Flysch | % Flint | % Ophiolite |
| Present channel |   |  | 8388            | 7                | 72.7  | 26.6     | 0.5     | 0.2         |
| Klithi unit     | Mean = 3.2<br>S.D. = 0.7<br>Range = 1.8–4.5         | 4.5                                    | 1139            | 2                | 69.3  | 29.6     | 1.0     | 0.1         |
| Vikos unit      | Mean = 6.8<br>S.D. = 1.7<br>Range = 3.9–9.7         | 8.3                                    | 695             | 2                | 82.3  | 12.8     | 0.6     | 4.3         |
| Aristi unit     | Mean = 12.4<br>S.D. = 3.9<br>Range = 6.7–25.9       | 25.9                                   | 5680            | 9                | 94.6  | 3.1      | 2.2     | 0.1         |
| Kipi unit       | 56  | 22.9                                   | 361             | 1                | 18.7  | 36.7     | 0.9     | 44.0        |

### Alluvial Sediment Sources

During the last glaciation the limestone headwaters of the Voidomatis basin (Tsepelovon district, Figure 16.1) supported valley glaciers, and huge amounts of limestone-rich sediment were supplied to the river system. The Late Würm Aristi unit is thus dominated by limestone gravels (94.6%) whereas the coarse sediment fraction of the late Holocene Klithi unit contains almost 30% flysch (Table 16.1). X-ray diffraction analyses have also highlighted the marked lithological contrast between the fine sediment loads of the cold stage, full-glacial Voidomatis (Aristi unit), which is rich in  $\text{CaCO}_3$ , and the fine sediment loads of the Klithi unit and modern fluvial systems which are composed largely of flysch-derived silts (Figure 16.4). The Vikos unit sediments are intermediate in composition between those of the Aristi unit and the modern floodplain sediments. The lithological composition of the post-Aristi alluvial units reflects the waning glacial input and the increase in erosion and sediment delivery from those parts of the catchment underlain by flysch rocks and soils. It can be shown that the relative proportions of flysch- and limestone-derived sediment in each of the alluvial units is a significant soil-forming factor and has implications for parent material composition and pedogenic weathering rates.

## DATA COLLECTION

### Field Sampling

Following a basin-wide geomorphological survey, five alluvial soil profiles (A to E) were selected for detailed study. These were located along a 6 km reach of the

Table 16.1 (Continued)

| Coarse (C)/<br>fine (F)<br>sediment<br>member ratio | Munsell<br>colour of<br><63 $\mu\text{m}$<br>fraction | Fluvial sedimentation style<br>and (in parentheses) the<br>dominant source of the<br>suspended sediment load       | Age of unit<br>(years BP)  |
|---|---|--|--|
| C > F   | yellowish<br>brown<br>10YR 5/8                        | Incising, confined meandering gravel bed<br>river. Low suspended sediment load.<br>(Flysch sediments)              | <30  |
| C $\leq$ F  | yellowish<br>brown<br>10YR 5/8                        | Aggrading, high sinuosity gravel bed river.<br>High suspended sediment load.<br>(Flysch sediments)                 | 1000 ( $\pm 50$ ) <sup>a</sup> -30   |
| C $\geq$ F  | brownish<br>yellow<br>10YR 6/8                        | Incising wandering gravel bed river.<br><br>Low suspended sediment load.<br>(Flysch and glacial sediments)         | 24 300 ( $\pm 2600$ ) <sup>b</sup> -<br>19 600 ( $\pm 200$ ) <sup>c</sup>  |
| C $\geq$ F  | very pale<br>brown<br>10 YR 8/7-4                     | Aggrading, low sinuosity, coarse sediment<br>river system.<br>High suspended sediment load.<br>(Glacial sediments) | 28 200 ( $\pm 7000$ ) <sup>c</sup> -<br>24 300 ( $\pm 2600$ ) <sup>b</sup> |
| C > F   | yellowish<br>brown<br>10YR 5/8                        | Aggrading (?) low sinuosity, coarse<br>sediment river system<br>(Flysch sediments)                                 | >150 000 <sup>c</sup>  |

Voidomatis River in the Lower Vikos Gorge and the southernmost margin of the Konitsa Plain (Figure 16.1 and Table 16.2). Profiles B and D are located approximately 40 m and 100 m respectively immediately downstream of the Old Klithonia Bridge at which point the Voidomatis leaves the confines of the Lower Vikos Gorge. To minimise any site-dependent variations in soil profile character, the sections under investigation are all situated in right-bank, free-draining portions of terraced alluvial sediments away from the main gorge walls, major talus formations and tributary junctions. Soil samples (*c.* 150–200 g) were collected, mostly at 10 cm intervals, from the terrace surface down to unweathered or least altered parent material (C horizon). Sixty-two sediment samples were collected from five soil profiles which ranged in depth from 0.6 to 2 m (Table 16.2).

**Table 16.2** Location of the soil profiles discussed in this chapter. The Quaternary alluvial units which form the parent material at each of these sites (A to E) are shown in Figure 16.1 and their lithological properties are summarised in Table 16.1

| Soil<br>profile | Parent<br>material | Location of profile<br>(see Figure 16.1) | Depth of<br>sampled<br>profile (cm) | Number<br>of soil<br>samples |
|-----------------|--------------------|--|-------------------------------------|------------------------------|
| A               | Aristi unit        | Papingo Bridge (4)                       | 200                                 | 20                           |
| B               | Aristi unit        | Old Klithonia Bridge (7)                 | 140                                 | 14                           |
| C               | Vikos unit         | 2 km downstream of Vikos (3)             | 100                                 | 10                           |
| D               | Klithi unit        | Old Klithonia Bridge (7)                 | 60                                  | 3                            |
| E               | Klithi unit        | Klithi (5)                               | 150                                 | 15                           |

### Laboratory Methods

All the sediment samples were air dried in the laboratory at room temperature for 48 hours prior to screening through a 1 mm mesh sieve. Calcium carbonate ( $\text{CaCO}_3$ ) and organic carbon (loss on ignition) determinations were made on bulk (<1 mm) samples following methods described by Gross (1971). The particle size characteristics of the fine sediment fraction (<63  $\mu\text{m}$ ) were measured using the computer-interfaced SediGraph 5000ET system reported by Jones *et al.* (1988). Low field magnetic susceptibility measurements were carried out on a mass specific basis using a standard Bartington system (Thompson and Oldfield, 1986) and total ferric iron present in oxyhydroxide phases such as haematite and goethite ( $\text{Fe}_2\text{O}_3d$ ) was determined using the dithionite–citrate–bicarbonate procedure described by Mehra and Jackson (1960).

## PEDOGENIC WEATHERING AND PROFILE DEVELOPMENT

Weathering takes place in soil profiles because minerals are only stable in the environment in which they form—following deposition in a new environment, minerals break down and liberate products which are in equilibrium with ambient soil chemistry (Pye, 1983).

### Climatic Regime and Profile Development

Climate is often the dominant influence upon the pedogenic weathering regime—controlling both the rate and degree of mineral alteration and thus ultimately regulating the properties of many soils. This climatic control can be viewed in terms of moisture delivery to the soil profile and near-surface temperature conditions. The volume of moisture to actually percolate into the soil profile (moisture throughput) controls the degree of edaphic activity, and regulates the intensity of weathering and leaching conditions, whilst temperature can influence the rate of chemical and biological processes in the soil. Increased leaching may result in the removal of bases and build-up of iron oxides, while a rise in temperature will accelerate the rate of formation of a particular mineral and therefore its abundance in profiles of a particular age (Catt, 1988). In contrast, in exceptionally arid environments, even the most mobile profile constituents can be retained in the upper soil and the development of illuvial horizons is severely retarded or prevented. Climate has a direct effect upon the type of soil profile that is formed.

### Parent Material Composition and Profile Development

Since different mineral species vary markedly in their resistance to surface weathering (cf. Curtis, 1976), the physical and chemical properties of parent sediments are also crucial factors in chronosequence development. Parent material lithology exerts an important influence upon the rate of operation of all weathering processes and the overall pace of profile development. For example, sediments containing easily weathered iron-bearing minerals may redden very quickly, while those containing

more resistant iron minerals may take longer to attain an equivalent degree of redness (Pye, 1983). Similarly, under free-draining, leaching conditions, parent materials with a comparatively low  $\text{CaCO}_3$  component may become decalcified fairly rapidly, allowing the pedogenic weathering front to penetrate downwards relatively quickly into the primary sediment, and will also contain a greater proportion of non-carbonate minerals available for subsequent modification. In other words, sediments, with many weatherable components will show more rapid weathering rates than sediments with less weatherable components.

By comparing profile depth functions between soils of different ages in the same locality, it is possible to observe the genesis and development of pedogenic features. A number of closely related processes operate to produce the pedogenic weathering regime of the Voidomatis Basin and these are described below.

### Organic Matter Translocation

Soil organic matter is derived from numerous sources including the terrace surface litter supply, the dissolved or suspended organic load from stemflow and the *in situ* decomposition of root material and soil organisms. The processes involved during the incorporation of organic material into the weathering profile are numerous and complex. In the Voidomatis alluvial soils, as is generally the case in most soil types, organic content tends to reach a fairly stable level first in the upper profile. The parent alluvial sediments contain little organic material. For example, unweathered C horizon sediments at the base of the Pleistocene sections have organic components of <2.5%. All the profiles are richer in organic matter at the soil surface, although these values are not related to soil age. Under certain conditions, however, the depth of organic-enriched horizons can provide a good indication of profile maturity. The accumulation of organic matter deep in the weathering profile appears to be encouraged by a climatic regime in which a period of moisture deficiency promotes aggregate shrinkage and vertical fracturing allowing finely comminuted humus and particulates to be translocated as colloidal suspensions from the upper soil. Following decalcification of the upper soil, this mechanism appears to be the dominant agency for the downward diffusion of organic matter in this environment. Only profiles A and B contain >7% organic material below 50 cm (Figure 16.5), while the younger Vikos and Klithi unit soils exhibit comparatively low values (<4%). This is because the pedogenic weathering front has not yet penetrated so deeply into their respective substrates. The build-up of organic matter in the illuvial B horizon appears to be a useful measure of relative age (Table 16.3).

### Leaching of Calcium Carbonate

The presence of  $\text{CaCO}_3$  in the soil matrix retards chemical weathering processes and restricts the vertical movement of fine particles.  $\text{CaCO}_3$  is progressively leached from the upper soil and this is the first major pedogenic alteration of the alluvial parent material. The effect of the leaching process over time is well illustrated by the increasing depth to carbonate in all five sections (Table 16.3). Profiles A to E are all free-draining sites which do not favour the reprecipitation of  $\text{CaCO}_3$  in the lower profile. The extent and depth of  $\text{CaCO}_3$  removal exerts an important control upon

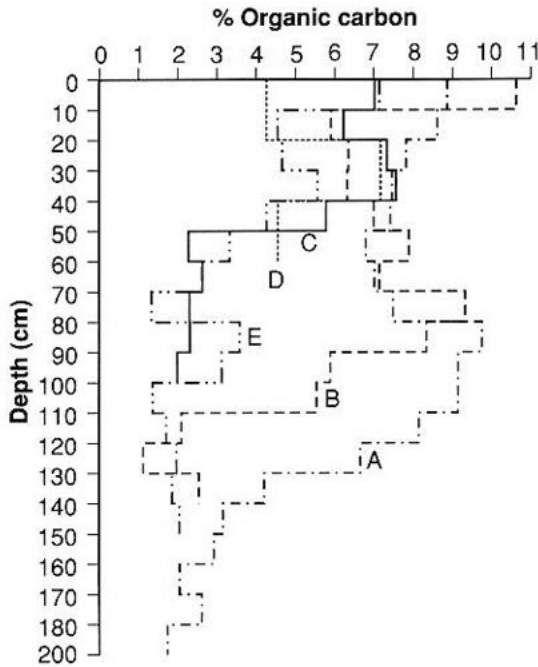


**Figure 16.5** Changes with depth in organic carbon content for all five profiles

soil pH and, therefore, upon the rate of breakdown of residual, non-carbonate mineral species. Secondary deposition of  $\text{CaCO}_3$  has not been observed in any of the studied profiles. Under the modern humid climatic regime, the high annual rainfall totals (>2000 mm) and the unconsolidated nature of the host sediment gravel matrix promote a vigorous and effective leaching zone in the upper soil. The amount of carbonate removal is greatest in the Pleistocene soils and, taking into consideration the original  $\text{CaCO}_3$  content of the parent sediment, there appears to be a straightforward relationship between depth to carbonate and soil age. The carbonate-free horizon at profile A is much deeper than the equivalent feature in the other soils suggesting that this soil is considerably older than the rest of the sequence.

### Clay Illuviation

According to Birkeland (1984), argillic horizon development is largely time-dependent since mineral breakdown and clay translocation are relatively slow processes. In the present study only the soils developed on the Vikos and Aristi alluvial units display B horizons containing clay-grade (<2  $\mu\text{m}$ ) material (Figure 16.6). Clays are absent from the parent materials for all the soils and the B horizon clays represent secondary accumulation. It is to be expected that soils developing in different parent materials will not produce B horizons at the same rate (Borchard and Hill, 1985) even if the starting materials in each case are clay-free. The crucial factors here are the mineralogical composition of the parent material and the clay-production potential

**Table 16.3** Selected soil parameters to illustrate the extent of pedogenic weathering in each of the profiles and the significance of parent material composition and time in profile development

| Soil profile | Depth to CaCO <sub>3</sub> (cm) | Thickness and depth of argillic B horizon (cm) | Finest median size ( $\phi$ ) of the fraction <63 $\mu$ m (and depth in cm) | Maximum organic content of B horizon (%) | Profile dithionite extractable iron maxima (mg kg <sup>-1</sup> ) (and depth in cm) | Mean magnetic susceptibility of top 60 cm (m <sup>3</sup> kg <sup>-1</sup> ) |
|--------------|---------------------------------|--|---|--|---|--|
| A            | 110                             | 140 (0-140)                                    | 8.98 (80-90)  | 9.76                                     | 24 090 (100-110)  | 238.5  |
| B            | 60                              | 50 (30-80)                                     | 6.23 (70-80)  | 9.33                                     | 18 170 (70-80)  | 95.2   |
| C            | 40                              | 30 (10-40)                                     | 6.98 (20-30)  | 7.56                                     | 18 610 (30-40)  | 128.7  |
| D            | 20                              | 0  | 5.52 (20-40)  | 7.17                                     | 12 590 (20-40)  | 65.2   |
| E            | 0                               | 0  | 5.32 (20-30)  | No B horizon                             | 7250 (30-40)  | 27.3   |



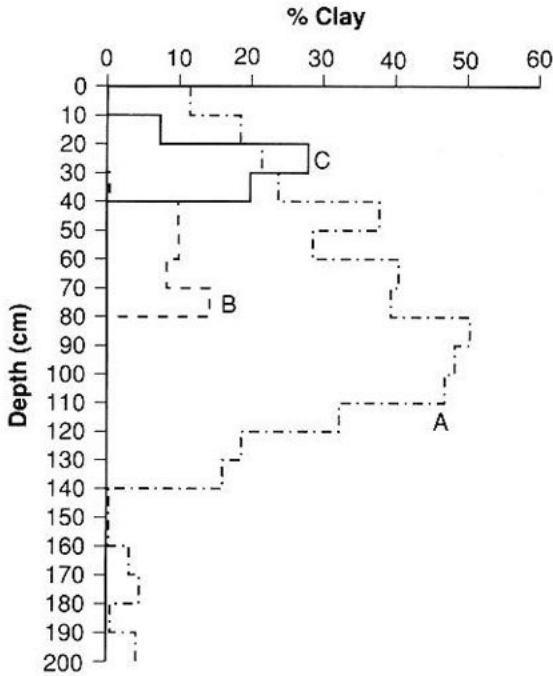


**Figure 16.6** Downprofile variations in clay content illustrating the extent of argillic *B* horizon development in the Pleistocene alluvial soils

of this mineral suite. Parent materials rich in  $\text{CaCO}_3$  (such as those of the Aristi unit) may contain only a comparatively low stock of clay-yielding minerals. Since in the present study, the parent materials are all free of clay-grade ( $<2 \mu\text{m}$ ) material, the extent of argillic *B* horizon development would seem to offer a useful guide to relative age. Only the pre-Holocene soils contain argillic horizons and these are shown in Figure 16.6. Several processes are involved in the development of such horizons, and the amount of illuvial clay in argillic horizons and their thickness is dependent on several factors. In general, however, a plot of clay content against depth usually shows an increase in the amount and in the thickness of *B* horizon clay with time (Birkeland, 1984). It is likely that the clay-rich *B* horizons evident in profiles A, B and C are the result of a number of processes including the *in situ* production of clay through mineral alteration as well as the incorporation of aeolian dust. The relative importance of these processes is difficult to determine; however, the extent of clay illuviation at site A is clearly much greater than at sites B and C, and provides further evidence to suggest that this soil is considerably older than the soils at the other two sites.

It is instructive to compare all five profiles using the median grain size of the fraction  $<63 \mu\text{m}$ . These depth functions are presented in Figure 16.7 and serve to highlight the time-dependent nature of fine sediment illuviation. The five median size profiles illustrate the evolution of the argillic *B* horizon as both the proportion of fines increases and the illuvial horizon thickens and moves deeper into the substrate over time. In very mature soils this development may also be accompanied by a thinning

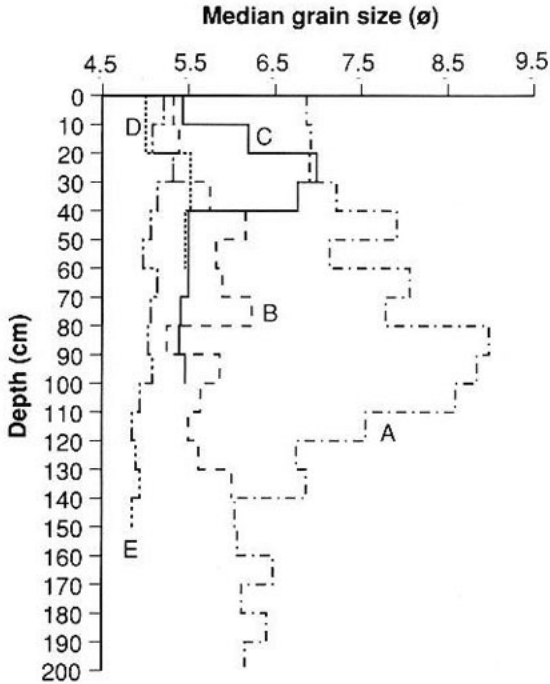


**Figure 16.7** Downprofile changes in median grain size of the fraction  $<63 \mu\text{m}$

of the *A* horizon (cf. McFadden and Weldon, 1987). This process could be indicative of a significant contribution from aeolian dust especially when the theoretical clay-production potential of elluvial horizons has been exceeded.

### Soil Iron Transformations

Numerous workers have documented the time-dependent nature of pedogenic iron accumulation in weathering profiles (e.g. McFadden and Hendricks, 1985). The terraced alluvial sediments of the Voidomatis basin promote free-draining conditions, and chemical weathering by oxidation takes place as ferrous iron-bearing minerals convert to insoluble ferric oxides or hydroxides. The results of this process are clearly evident in the Pleistocene soils of sites A, B and C which all show very considerable contrasts in total ferric iron ( $\text{Fe}_2\text{O}_3d$ ) content between the *C* and *B* horizons (Figure 16.8). Although profile E shows no evidence of such alteration, profile D evidences some iron oxide production in the *B* horizon (20–40 cm). The amount of  $\text{Fe}_2\text{O}_3d$  in profiles A, B, C and D is greatest in the *B* horizon and usually towards the base of this feature (Figure 16.8). Over time the ferrous iron component in the parent mineral suite is progressively converted to ferric iron and in the Voidomatis soils total ferric iron and the depth and thickness of the iron-enriched illuvial horizon seems to provide a useful measure of relative age (Table 16.3).

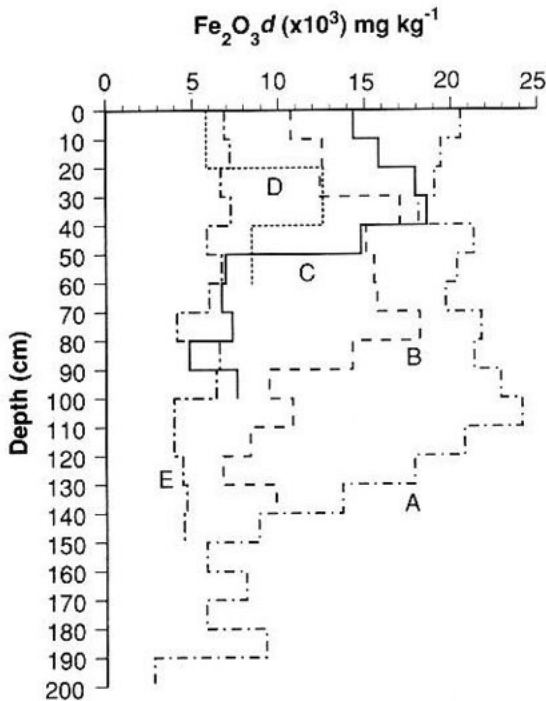


**Figure 16.8** Downprofile changes in total iron oxide ( $\text{Fe}_2\text{O}_3d$ ) content in each of the studied profiles

### Magnetic Susceptibility Horization

There is a strong positive correlation between the amount of ferric iron present and the magnetic susceptibility of the soil samples. Indeed, the observed pattern of magnetic enhancement is closely related to the pedogenic transformation of iron-bearing compounds (see Dearing *et al.*, 1985). The production of magnetic minerals by pedogenic weathering is similarly time-dependent and a positive relationship exists between magnetic susceptibility and profile age. This general trend is again modified by the influence of parent material composition. Those substrates richer in flysch-derived materials (profiles C, D and E) contain a greater proportion of non-carbonate minerals available for the *in situ* production of magnetic minerals by pedogenesis. Profile E on the Klithi unit has a relatively constant downprofile magnetic signature (range 18 to  $30.3 \text{ m}^3 \text{ kg}^{-1}$ ) with a mean value of  $23.8 \text{ m}^3 \text{ kg}^{-1}$ . Profile B (Late Pleistocene) has a 50 cm thick clay-rich B horizon, yet profile D (late Holocene) displays a very similar magnetic susceptibility maxima to that of B at depths between 20 and 40 cm (Figure 16.9).

The Voidomatis soils also display the characteristic feature of topsoil magnetic enhancement which has been documented by several authors, although the actual processes responsible are still not fully understood (Thompson and Oldfield, 1986). Providing the magnetic properties of the parent sediments are known, the magnetic

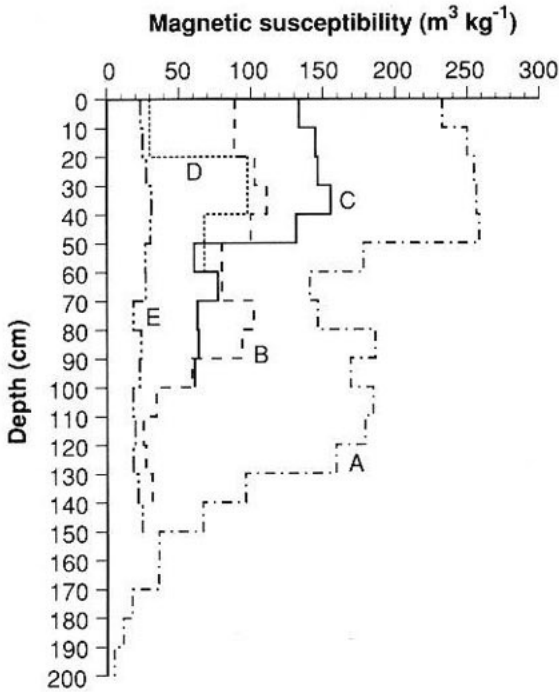


**Figure 16.9** Downprofile changes in low frequency magnetic susceptibility

susceptibility of illuvial horizons provides a useful indication of soil age (Singer *et al.*, 1992).

## THE VOIDOMATIS CHRONOSEQUENCE

### The Klithi Alluvial Unit

The sediments at profile E were deposited within the present century (Lewin *et al.*, 1991) and show no evidence of pedogenic weathering. Apart from this most recent alluvial unit, all the soils have decalcified upper horizons, and the respective depths to carbonate are shown in Table 16.3. The magnetic susceptibility and median size data for profile E show no marked downprofile variation. In contrast, profile D, located on the southernmost part of the Konitsa Plain, has a decalcified upper horizon (20 cm), and the magnetic susceptibility and total ferric iron depth functions indicate some pedogenic alteration, although mineral weathering has not been sufficient to liberate clay-grade ( $<2 \mu\text{m}$ ) material. Organic deposits in an equivalent section approximately 100 m upstream of site E have been radiocarbon dated as modern ( $102.7 \pm 1.2\%$ , OxA-1747). However, Klithi unit sediments on the Konitsa Plain have yielded  $^{14}\text{C}$  dates of  $800 \pm 100$  (OxA-192) and  $1000 \pm 50$  (OxA-191) years BP

(Woodward *et al.*, 1992). The pedogenic weathering profiles thus corroborate the  $^{14}\text{C}$  dating evidence by indicating the continued development of the Klithi unit until quite recent times.

### The Vikos and Aristi Alluvial Units

The soil profile on the Vikos alluvial unit at site C includes an argillic *B* horizon 30 cm in thickness and pedogenic weathering is evident only in the upper 50 cm of this profile. Due to the significant flysch component in the parent material (Figure 16.4 and Table 16.1), the magnetic susceptibility and clay values in the *B* horizon actually exceed those of the profile at site B. However, on both stratigraphical and morphological grounds, as well as TL and ESR datings (see Figure 16.1 and Table 16.1) the alluvial sediments at site B clearly predate those at profile C. This scheme is supported by their respective weathering profiles. The argillic *B* horizon at site B is thicker and located deeper in the profile than at site C, and organic material has been translocated down to a depth of 110 cm. The observed differences in degree of pedogenic weathering are thus attributable primarily to age and secondly to contrasts in parent material composition. Some further examples of this pattern are shown in Table 16.3 and Figure 16.10. Profiles C and D have developed in parent sediments with a significant flysch component, and therefore contain a greater proportion of non-carbonate minerals available for pedogenic modification. The availability of a greater proportion of weatherable minerals allows illuvial horizons to develop relatively rapidly.

It is clear from Figure 16.6 that the argillic *B* horizon of profile A is much thicker and richer in clay than the other soils in the basin. This supports the observed pattern of  $\text{CaCO}_3$  removal by also suggesting that soil profile A is considerably older than profile B. Indeed, it is unlikely that the large difference in clay accumulation could be attributed solely to site-dependent factors since both profiles are developed in free-draining, glacio-fluvial gravels in very similar topographic settings. The exposures at both sites A and B are capped by a distinctive, strongly weathered fine member approximately 70 cm in thickness, which immediately overlies coarse, cobble- to boulder-sized limestone gravels (Figure 16.11). The pedogenic weathering front at profile A is, however, considerably deeper and has penetrated the base of this fine member.

The extent of parent material alteration in each of the studied profiles may be further illustrated by means of the plots shown in Figure 16.12. These portray the maximum and minimum values of the parameters shown for each of the five profiles. The gradient of the line for each profile provides a useful illustration of the difference between the parent material and the most strongly altered horizons. In each case profile E displays a relatively flat line indicating little or no alteration, whereas profile A always evidences the greatest difference. The data for profile E provide a useful guide for the possible degree of at-a-site primary variability in the data set. It is interesting to note that in each of the examples shown, the maximum values lie in the same sequence: A, C, B, D and E, whereas the actual age-scheme from oldest to youngest is A, B, C, D and E. This further highlights the influence of parent material composition on these three parameters for this particular alluvial chronosequence.

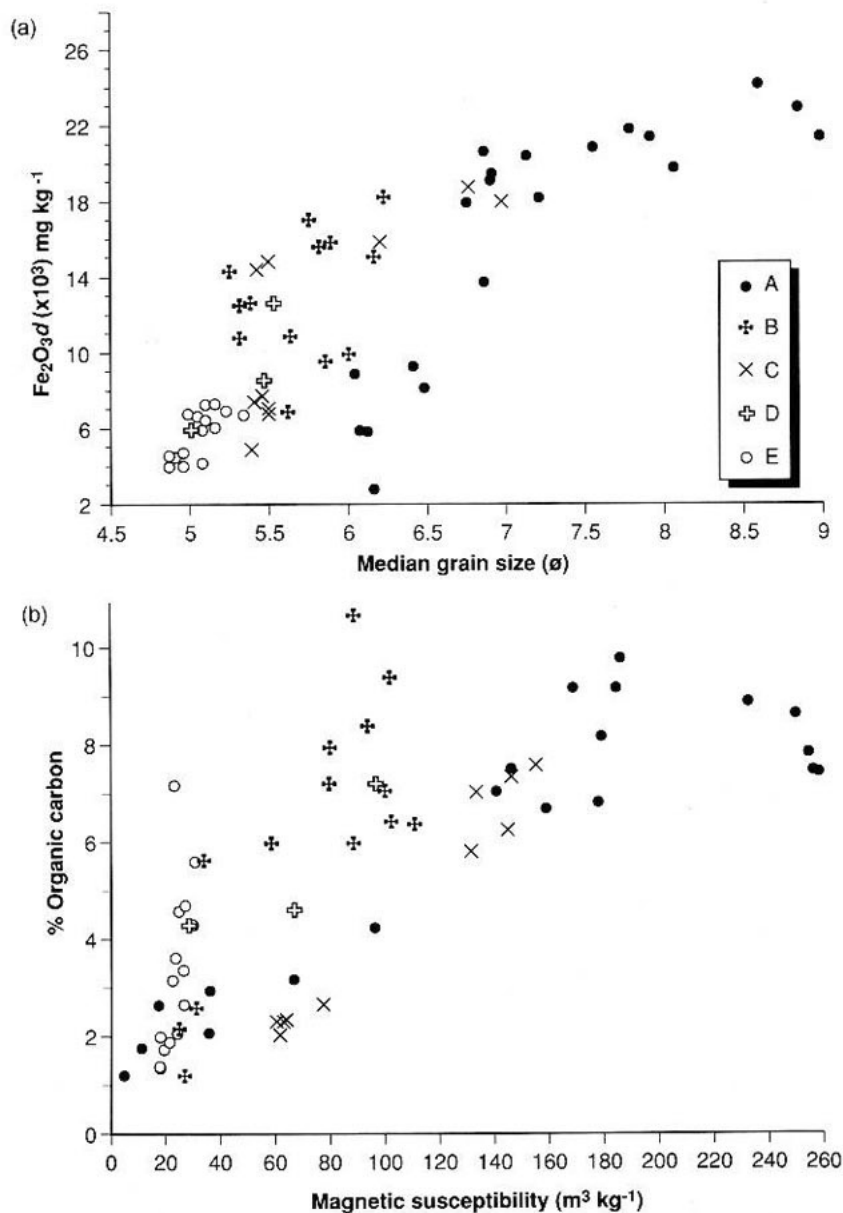


**Figure 16.10** Bivariate plots showing the relationship between (a) Fe<sub>2</sub>O<sub>3d</sub> content and median grain size, and (b) % organic carbon and magnetic susceptibility in all five weathering profiles. These plots further highlight the dual influence of time and parent material composition on the pattern of pedogenic alteration

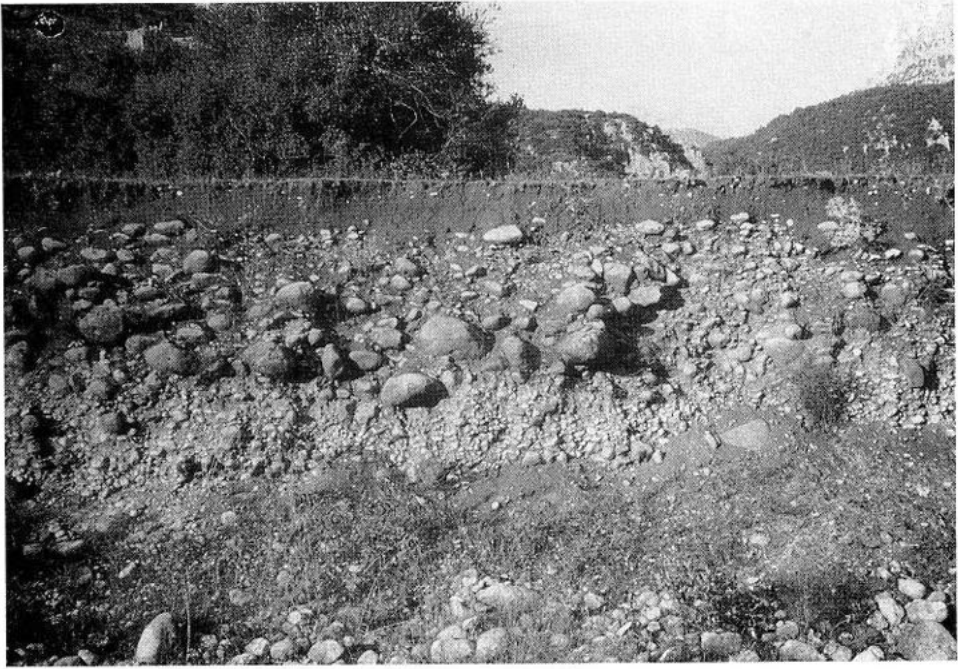


**Figure 16.11** Soil profile A in the Lower Vikos Gorge. The fine-grained member capping this section is approximately 70 cm in thickness. This photograph shows a typical section in the coarse, limestone-rich glacio-fluvial gravels of the Aristi unit

In a recent paper Veldkamp and Feijtel (1992) have attempted to evaluate the influence of parent material composition on subsoil weathering rates in the Allier terrace chronosequence of central France. They simulated long-term (several hundred thousands of years) weathering patterns using a simple process model and concluded that the role of parent material controlled weathering is only prominent in ‘young’ sediments with many weatherable fragments and that, after prolonged weathering, this influence diminishes. Such a process may partly explain the comparatively rapid development of the Vikos unit (C) and Klithi unit (D) soils, each of which contains a much greater proportion of flysch-derived fine sediment than the Aristi unit profiles (Figure 16.4).

### **A Pedogenic Weathering Index**

Using the iron oxide data presented in Figure 16.8 a simple weathering index has been developed incorporating information on both the degree of pedogenic transformation within each profile (relative to parent material composition) and the thickness of the weathered zone. This index is the product of the difference between the maximum  $\text{Fe}_2\text{O}_3d$  values and the least-altered or unweathered sample values at the base of each profile ( $\text{mg kg}^{-1}$ ) and the total thickness (m) of the strongly weathered horizon. These values have been plotted against the ages of the alluvial units (Table 16.1) and are

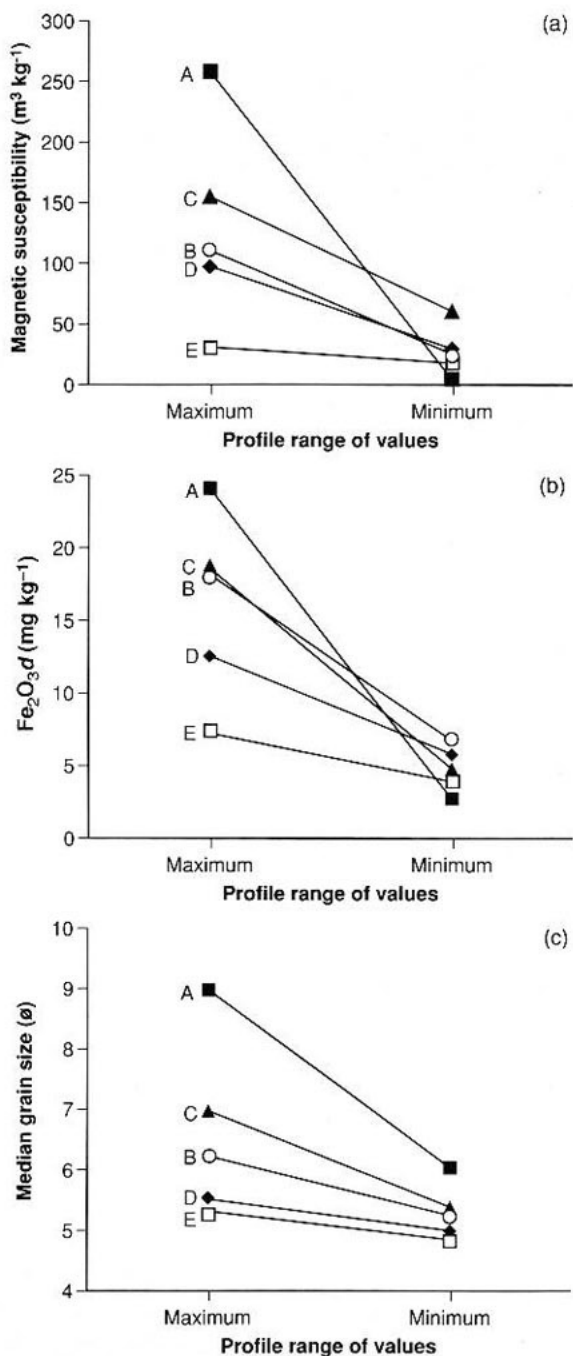


**Figure 16.12** Maximum and minimum values of (a) low frequency magnetic susceptibility, (b) iron oxide ( $\text{Fe}_2\text{O}_3\text{d} \times 10^3$ ) and (c) median grain size of the fraction  $<63 \mu\text{m}$  for each of the soil profiles



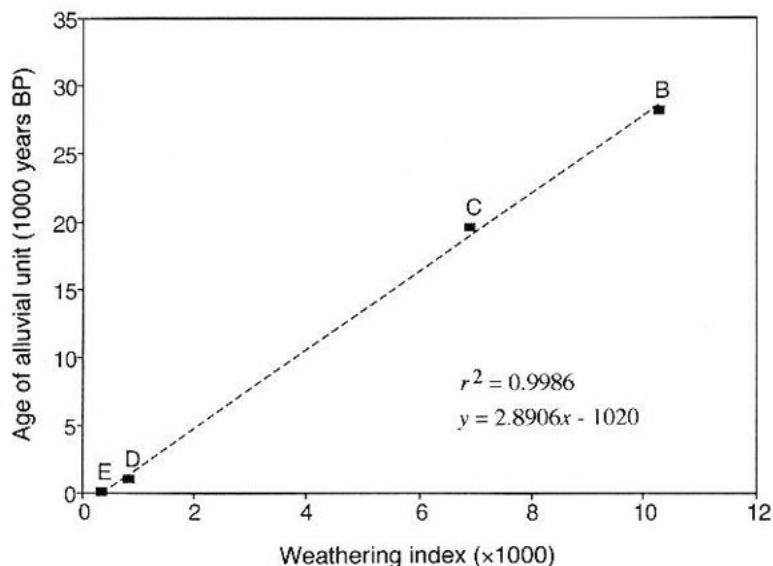


**Figure 16.13** The relationship between soil profile age (see Table 16.1) and the weathering index derived from the iron oxide ( $\text{Fe}_2\text{O}_3d$ ) data (see text for explanation)

shown in Figure 16.13. Using this relationship the index score for profile A gives an estimated age of *c.* 85 000 years BP which places this aggradational phase and the glacial activity to which it relates early in the last cold stage. However, this age estimate must be regarded as a minimum as we do not know if the relationship between this weathering index and profile age is truly linear in this environment for profiles older than profile B. Indeed, many studies have highlighted how weathering rates tend to slow down with the passage of time (e.g. Birkeland, 1984; Bull, 1991; Swanson *et al.*, 1993). We would like to stress that this age-estimate is preliminary and should be regarded as a minimum. It is quite possible that profile A actually predates the Last Interglacial, and at present it is only possible to say with certainty that profile A represents an episode of glacial activity which predates the last major (Late Würm) ice advance in the Pindus Mountains.

## IMPLICATIONS FOR THE GLACIAL HISTORY OF NORTHWEST GREECE

The alluvial sediments at profile B (Old Klithonia Bridge) have been dated to between 28 000 and 24 300 years BP (Table 16.1), indicating that deposition took place towards the end of the last glacial period (Bailey *et al.*, 1990; Lewin *et al.*, 1991). In contrast, the alluvial sediments at profile A (Papingo Bridge) have not been dated by TL or ESR and the soil developed at this site is clearly the oldest of the five studied profiles. Moreover, the extent of pedogenic weathering at this site (relative to site B) implies that these river sediments are considerably older than the last glacial maximum. All the measured parameters indicate that profile A is considerably older than the rest

of the sequence. To date, despite extensive field survey, profile A is the only location in the catchment where we have found evidence of such strongly weathered Aristi unit sediments.

This is perhaps not surprising, since these deposits are located on the inside of a large meander some distance (250 m) from the contemporary floodplain system in the widest section of the Lower Vikos Gorge (Figure 16.2). This body of sediment has thus been protected from fluvial erosion. Elsewhere in the basin the main gorge is much narrower and the modern river is vigorously reworking Pleistocene and more recent alluvium, as well as actively undercutting limestone bedrock walls at many locations. It seems likely that most of the earlier alluvium has been eroded away. Residence times for alluvium in such high-energy gorge environments can be relatively brief—rapid reworking is common, especially in narrow bedrock reaches where increases in discharge during major flood events are accompanied by large increases in river stage and stream power.

The most significant outcome of this pedogenic weathering investigation is the subdivision of the Aristi unit into two distinct alluvial units. Each of these is composed of glacially-derived sediments with similar lithological properties. It has been suggested previously that the large amount of clay present in profile A may partly reflect the incorporation of aeolian dust as well as *in situ* breakdown of clay-yielding minerals. This seems to be a plausible mechanism since this terrace surface could have been exposed to sub-aerial processes throughout the last glacial period.

## CONCLUSIONS

During the Quaternary Period, phases of valley alluviation in the Voidomatis basin were followed by episodes of downcutting, and pedogenic weathering took place on stable terrace surfaces. The alluvial soils described in this paper have formed under long periods of seasonal leaching in a free-draining, oxidising environment. These soil profiles display significant differences in decalcification depth, amount of clay illuviation, total iron oxide content, and B horizon organic matter accumulation. All these features can be attributed primarily to differences in soil profile age—although interprofile contrasts in parent material composition have been sufficient to slightly modify this trend.

The relative-age sequence derived from soil profile development corroborates the model of alluvial history reported by Lewin *et al.* (1991). However, there is now evidence to suggest that the alluvial parent material at soil profile A may derive from an episode of Pleistocene glacial activity which predates the Late Würm Aristi unit at soil profile B (c. 28 200 to 24 300 years BP). It now seems likely, therefore, that the northern Pindus Mountains were also glaciated before the last major (Late Würm) ice advance and that at least two major phases of glacial activity can now be recognised in the Greek Pleistocene. Further work is in progress to test this implication.

In a wider context, this study has attempted to demonstrate how, in certain environments, sediments and landforms of markedly different ages can often be indistinguishable when only primary lithological properties and altitudinal criteria are employed. Despite recent major advances in the application and refinement of

physical dating techniques such as ESR, luminescence and AMS  $^{14}\text{C}$ , in the absence of datable materials, weathering profiles may provide the only available means of differentiating between otherwise similar deposits. Increasing awareness of the inherently homotaxial nature of the Quaternary rock record (Bowen, 1991) should ensure that relative-age estimates based upon measurable patterns of pedogenic weathering will continue to play an important role in studies of Quaternary landscape evolution.

## ACKNOWLEDGEMENTS

This work was carried out while JCW held a SERC Ph.D. studentship at Darwin College and the Subdepartment of Quaternary Research (Godwin Laboratory) at the University of Cambridge. We would especially like to thank Geoff Bailey and all the members of the Klithi Archaeological Project for their support and also IGME (Athens) for permission to undertake fieldwork in Epirus. We also thank Watts Stelling for iron oxide analyses, Simon Robinson for assistance with magnetic susceptibility measurements and the sedimentology laboratory in the Department of Earth Sciences in Cambridge for generously allowing access to the SediGraph and XRD facilities. The support of the British Geomorphological Research Group through the provision of a research grant to JCW for work on SPOT satellite imagery of NW Greece is also gratefully acknowledged. Terry Bacon and Andrew Teed of the Department of Geography at the University of Exeter kindly prepared the diagrams and photographs.

## REFERENCES

- Bailey, G. N., Lewin, J., Macklin, M. G. and Woodward, J. C. (1990). The "Older Fill" of the Voidomatis Valley Northwest Greece and its relationship to the Palaeolithic archaeology and glacial history of the region. *Journal of Archaeological Science*, **17**, 145–150.
- Bailey, G. N., Carter, P. L., Gamble, C. S., Higgs, H. P. and Roubet, C. (1984). Palaeolithic investigations in Epirus: the results of the first season's excavations at Klithi, 1983. *Annual of the British School of Archaeology at Athens*, **79**, 7–22.
- Bailey, G. N., Gamble, C. S., Higgs, H. P., Roubet, C., Sturdy, D. A. and Webley, D. P. (1986). Palaeolithic investigations at Klithi: preliminary results of the 1984–1985 field seasons. *Annual of the British School of Archaeology at Athens*, **81**, 7–35.
- Birkeland, P. W., (1982). Subdivision of Holocene glacial deposits, Ben Ohau Range, New Zealand, using relative-dating methods. *Geological Society of America Bulletin*, **93**, 433–449.
- Birkeland, P. W. (1984). *Soils and Geomorphology*. Oxford University Press, New York.
- Boardman, J. (1985). *Soils and Quaternary Landscape Evolution*. Wiley, Chichester.
- Borchard, G. and Hill, R. L. (1985). Smectitic pedogenesis and late Holocene tectonism along the Raymond Fault, San Marino, California. In Weide, D. L. (ed.), *Soils and Quaternary Geology of the Southwestern United States*, Geological Survey of America Special Paper No. 203.
- Bowen, D. Q. (1991). Glacial sediment systems. In Ehlers, J., Gibbard, P. L. and Rose, J. (eds), *Glacial Deposits in Great Britain and Ireland*, Balkema, Rotterdam, pp. 3–11.
- Büdel, J. (1982). *Climatic Geomorphology*. Princeton University Press, Princeton.
- Bull, W. B. (1991). *Geomorphic Responses to Climatic Change*. Oxford University Press, Oxford.
- Catt, J. A. (1986). *Soils and Quaternary Geology: A Handbook for Field Scientists*. Clarendon Press, Oxford.
- Catt, J. A. (1988). Soils of the Plio-Pleistocene: do they distinguish types of interglacial? In Shackleton, N. J., West, R. G. and Bowen, D. Q. (eds), *The Past Three Million Years: Evolution of Climatic Variability in the North Atlantic Region*, Royal Society of London, pp. 539–557.

- Colman, S. M. and Pierce, K. L. (1986). Glacial sequence near McCall, Idaho: Weathering rinds, soil development, morphology and other relative age criteria. *Quaternary Research*, **25**, 25–42.
- Curtis, C. D. (1976). Stability of minerals in surface weathering reactions: a general thermochemical approach. *Earth Surface Processes*, **1**, 63–70.
- Dearing, J. A., Maher, B. A. and Oldfield, F. (1985). Geomorphological linkages between soils and sediments: the role of magnetic measurements. In Richards, K. S., Arnett, R. R. and Ellis, S. (eds), *Geomorphology and Soils*, Allen and Unwin, London, pp. 245–266.
- Furlan, D. (1977). The climate of southeast Europe. In Wallen, C. C. (ed), *Climates of Central and Southern Europe*, Elsevier, Amsterdam, pp. 185–223.
- Gross, M. G. (1971). Carbon determination. In Carver, R. E. (ed.), *Procedures in Sedimentary Petrology*. Wiley, New York, pp. 541–569.
- Huttary, J. (1950). Die Verteilung der Niederschläge auf die Jahreszeiten im Mittelmeergebiet. *Meteorologische Rundschau*, **3**, 111–119.
- Jones, K. P. N., McCave, I. N. and Patel, P. D. (1988). A computer-interfaced sedigraph for modal size analysis of fine-grained sediment. *Sedimentology*, **35**, 163–172.
- Kemp, R. A. (1987). The interpretation and environmental significance of a buried Middle Pleistocene soil near Ipswich Airport, Suffolk, England. *Philosophical Transactions of the Royal Society of London*, **B317**, 365–391.
- Kukla, G. (1987). Loess Stratigraphy in Central China. *Quaternary Science Reviews*, **6**, 191–219.
- Lewin, J., Macklin, M. G. and Woodward, J. C. (1991). Late Quaternary fluvial sedimentation in the Voidomatis Basin, Epirus, northwest Greece. *Quaternary Research*, **35**, 103–115.
- McFadden, L. D. and Hendricks, D. M. (1985). Changes in the content and composition of pedogenic iron oxyhydroxides in a chronosequence of soils in southern California. *Quaternary Research*, **23**, 189–204.
- McFadden, L. D. and Weldon, R. J. (1987). Rates and processes of soil development on Quaternary terraces in Cajon Pass, California. *Geological Society of America Bulletin*, **98**, 280–293.
- Mehra, O. P. and Jackson, M. L. (1960). Iron oxide removal from soils and clays by a dithionite-citrate system buffered with sodium bicarbonate. *Proceedings of the 7th National Conference on Clays and Clay Minerals*, Pergamon, New York, pp. 317–327.
- Pye, K. (1983). Red beds. In Goudie, A. S. and Pye, K. (eds), *Chemical Sediments and Geomorphology*, Academic Press, London, pp. 227–263.
- Rose, J., Boardman, J., Kemp, R. A. and Whiteman, C. (1985). Palaeosols and the interpretation of the British Quaternary stratigraphy. In Richards, K. S., Arnett, R. R. and Ellis, S. (eds), *Geomorphology and Soils*, Allen and Unwin, London, pp. 348–375.
- Singer, M. J., Fine, P., Verosub, K. L. and Chadick, O. A. (1992). Time dependence of magnetic susceptibility of soil chronosequences on the California coast. *Quaternary Research*, **37**, 323–332.
- Statham, I. (1977). *Earth Surface Sediment Transport*. Oxford University Press, Oxford.
- Swanson, T. W., Elliott-Fisk, D. L. and Southard, R. J. (1993). Soil development parameters in the absence of a chronosequence in a glaciated basin of the White Mountains, California–Nevada. *Quaternary Research*, **39**, 186–200.
- Thompson, R. and Oldfield F. (1986). *Environmental Magnetism*. Allen and Unwin, London.
- Veldkamp, A. and Feijtel, T. C. (1992). Parent material controlled subsoil weathering in a chronosequence, the Allier terraces, Limagne rift valley, France. *Catena*, **19**, 475–489.
- Walter, H. and Leith, H. (1960). *Klimadiagramm-Weltatlas*. Jena.
- Weide, D. L. (1985). *Soils and Quaternary Geology of the Southwestern United States*. Geological Survey of America, Special Paper No. 203.
- Woodward, J. C. (1990). *Late Quaternary Sedimentary Environments in the Voidomatis Basin, Northwest Greece*, Unpublished Ph.D Thesis. University of Cambridge.
- Woodward, J. C., Lewin, J. and Macklin, M. G. (1992). Alluvial sediment sources in a glaciated catchment: the Voidomatis Basin, northwest Greece. *Earth Surface Processes and Landforms*, **16**, 205–216.